| Surrogate Signals | Patient 1 | | | | Patient 2 | | | |
|---|---|---|---|---|---|---|---|---|
| | Mean (mm) | Std (mm) | Max (mm) | 95$^{th}$%tile (mm) | Mean (mm) | Std (mm) | Max (mm) | 95$^{th}$%tile (mm) |
| Diaphragm signal + its temporal derivative | 0.64 | 0.44 | 4.57 | 1.47 | 0.67 | 0.67 | 6.61 | 2.09 |
| Skin signal + its temporal derivative | 0.97 | 0.89 | 7.07 | 2.85 | 0.68 | 0.69 | 6.35 | 2.17 |
| Mean image intensity + its temporal derivative | 0.94 | 0.77 | 6.61 | 2.54 | 0.91 | 0.82 | 8.82 | 2.65 |
| Image entropy + its temporal derivative | 1.07 | 0.93 | 9.90 | 3.04 | 0.8 | 0.77 | 7.26 | 2.45 |
| Scores of the 1$^{st}$ PC + its temporal derivative | 0.65 | 0.45 | 4.06 | 1.50 | 0.75 | 0.74 | 7.01 | 2.36 |
| Diaphragm signal + skin signal | 0.56 | 0.44 | 4.87 | 1.43 | 0.66 | 0.65 | 5.93 | 2.06 |
| Scores of the 1$^{st}$ PC + scores of the 2$^{nd}$ PC | 0.63 | 0.46 | 5.75 | 1.51 | 0.61 | 0.61 | 7.30 | 1.91 |
| Scores of the 1$^{st}$ PC + scores of the 3$^{rd}$ PC | 0.53 | 0.38 | 4.09 | 1.25 | 0.76 | 0.76 | 6.76 | 2.41 |
| Scores of the 1$^{st}$ PC + scores of the 2$^{nd}$ PC + scores of the 3$^{rd}$ PC | 0.49 | 0.35 | 3.85 | 1.17 | 0.59 | 0.59 | 7.06 | 1.85 |

Table 1. Summary statistics for the L2 norm of the DFE for all surrogate signals investigated to drive motion models for both patients. The mean, standard deviation and 95$^{th}$ percentile DFE values over all pixels were averaged over all test images, while the maximum DFE value over all test images was considered for the maximum values over all pixels. The scores of the 1$^{st}$, 2$^{nd}$ and, 3$^{rd}$ PC were obtained applying PCA to the image intensities.

**Conclusion**

PCA applied to the image intensities provides MRI-derived surrogate signals that give good results when modelling the 2D motion of the internal anatomy from a single slice. Future work will investigate other methods to generate surrogate signals, such as PCA applied to the DVF, and will use additional 2D datasets from more lung cancer patients. Furthermore, the surrogate-driven motion models will be extended to include the 3D motion of the full anatomy enabling retrospective off-line estimation of the actual delivered dose.

## OC-0412 Mechanically-assisted and non-invasive ventilation: Innovative step forward in the motion management

G. Van Ooteghem[1,2], D. Dasnoy-Sumell[3], G. Lemaire[4], G. Liistro[5], E. Sterpin[1], X. Geets[1,2]

[1]*Université Catholique de Louvain UCL - Institut de Recherche Expérimentale et Clinique IREC, SSS/IREC/MIRO Molecular Imaging- Radiotherapy and Oncology, Brussels, Belgium*

[2]*Cliniques Universitaires Saint Luc, Radiation Oncology, Brussels, Belgium*

[3]*Université Catholique de Louvain UCL, ImagX-R, Louvain-La-Neuve, Belgium*

[4]*Cliniques Universitaires Saint Luc, Anesthesiology, Brussels, Belgium*

[5]*Cliniques Universitaires Saint Luc, Pneumology, Brussels, Belgium*

**Purpose or Objective**

Management of breathing-related motion remains challenging. Current strategies rely either on dedicated margins (ITV, MidPosition) that result in futile irradiation of normal tissues, or on respiratory-synchronized techniques that are highly sensitive to changes in breathing pattern and technologically exacting. Therefore, mechanically-assisted and non-invasive ventilation (MANIV) could be used on unsedated patients to impose regular breathing and reproducible tumour motion, but also to modulate the breathing pattern for motion mitigation techniques. We investigated the feasibility of MANIV on volunteers, and its impact on internal motion.

**Material and Methods**

Twelve healthy volunteers underwent 2 sessions of dynamic MRI, repeated over a few days. Each session was divided in 4 acquisitions of 15 minutes with 4 ventilation modes: spontaneous mode (SP), volume-controlled mode (VC) that imposes regular breathing in physiologic conditions, shallow-controlled mode (SH) that intends to lower motion amplitudes when increasing the breathing rate up to 30 breaths per minute, and slow-controlled mode (SL) that mimics repeated end-inspiratory breath-holds (Figure 1). The last 3 modes were achieved under respirator without sedation. The motion of the diaphragm was tracked and expressed in position, amplitude, period and plateau during each MRI (intra-session analysis) and between MRI (inter-session analysis).

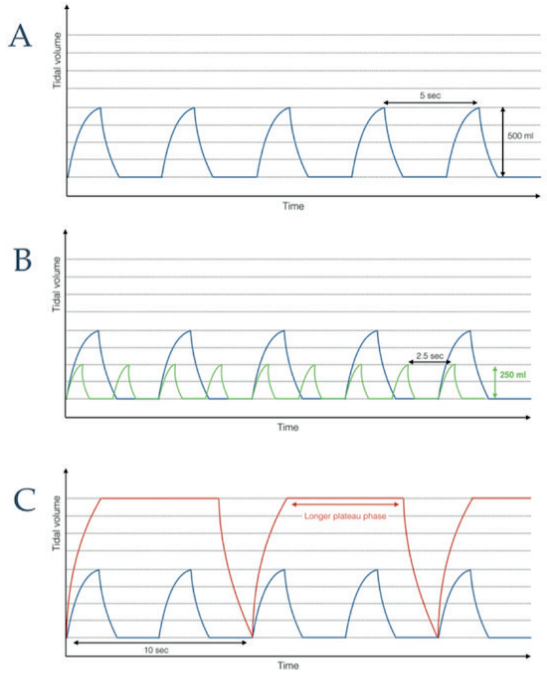


Figure 1 : (A) VC imposes a regular breathing rate and inhale volumes. (B) Increased breathing rate in SH allows smaller inhale volumes. (C) The end-inspiratory plateau in SL mimics repeated breath-holds.

**Results**

Intra-session analysis: Breathing rate variation was reduced in 97.92 % of cases with VC and SH compared to SP, with a mean reduction of 61.84 % ± 22.23. The mean amplitude variation was decreased in 62.5 % of cases. Furthermore, amplitudes were systematically reduced with SH compared to VC, with a mean reduction of 12.22 mm ± 6.4 (range: 5.2 – 27 mm) (Figure 2). In the SL mode, the mean variation of the plateau position was 4.84 mm ± 3.53 (range: 2.27 to 12.72 mm) with 66.66 % of the volunteers achieving a variation smaller than 5 mm.

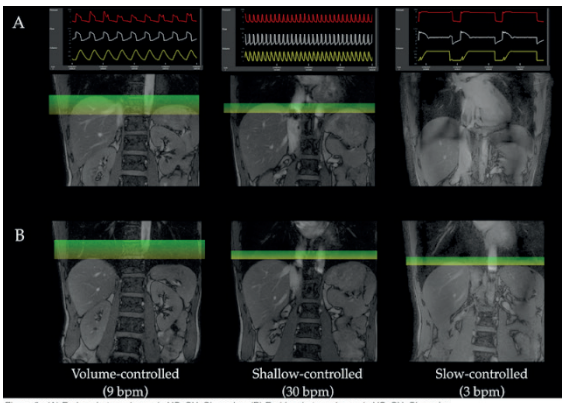


Figure 2 : (A) End-expiratory phases in VC, SH, SL modes. (B) End-inspiratory phases in VC, SH, SL modes. The green windows highlight the smaller amplitude obtained with the SH mode compared to the VC mode and the residual motion during the end-inspiratory plateau with the SL mode.

Inter-session analysis: Compared to SP, VC and SH reduced both the mean breathing rate variation (0.72 vs 0.01 and 0.02 sec, respectively) and the mean amplitude variation (3.6 vs 2.51 and 1.78 mm, respectively) between the two MRI sessions. For SL, the mean variation of the plateau positions was 6.08 mm ± 6.03 (range: 0.08

- 17.22 mm) with 58,33 % of the volunteers achieving a variation smaller than 5 mm.
MANIV was well-tolerated by all volunteers, without adverse event. The MRI environment led to more discomfort than MANIV itself.

**Conclusion**

MANIV offers exciting perspectives for motion management. It improves intra- and inter-session reproducibility of key motion characteristics, and should facilitate respiratory tracking (VC), gating (SL) and motion reduction techniques (SH). Since the volunteers had already regular spontaneous breathing, a larger gain is expected for real patients with poorer medical conditions. Studies on patients with thoracic, breast and upper-abdominal tumours are ongoing.

## OC-0413 4DCT and VMAT for lung patients with irregular breathing: Phase vs. amplitude binning

R. Caines[1], N. Sisson[1], C. Rowbottom[1]
[1]*The Clatterbridge Cancer Centre, Medical Physics, Liverpool, United Kingdom*

**Purpose or Objective**

Our recent study showed 4DCT was superior to 3DCT for VMAT planning of lung patients with irregular breathing. This study aims to evaluate for 4DCT whether phase- or amplitude-based binning is preferable.
Our objectives were to determine if, for irregularly breathing patients, phase or amplitude binning:

1. better represents tumour motion range
2. better represents average densities in the patient
3. better allows for VMAT plans delivered with acceptable dosimetric accuracy

**Material and Methods**

10 patient breathing traces were identified featuring irregularity in both phase and amplitude (e.g. Figure 1). Traces were fed to a programmable moving platform (max. sup-inf amplitude 2.85 cm) on which a CIRS lung tumour phantom was mounted, with two spherical tumours of 2 and 3 cm diameter. Expected tumour motion range and average density profiles were calculated from the breathing traces, together with HU values from a static scan.

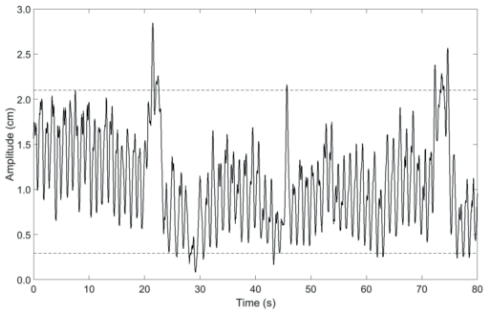


*Figure 1 Example irregular breathing trace. Dashed lines show middle 95% of amplitude distribution.*

4D scans were acquired for each breathing trace using a Philips Brilliance Big Bore CT with Varian RGSC respiratory monitoring. Scans were reconstructed from 6 bins equally spaced in (1) phase and (2) amplitude. ITVs were delineated on 4D-MIPs by HU thresholding, and tumour motion range measured. HU tumour profiles were extracted from 4D-AIPs, and agreement with expected profiles quantified by area-under-curve scoring.
PTVs were created on the 4D-AIPs for the 2 cm tumour using a 0.8 cm sup-inf ITV-PTV margin. Clinically representative VMAT plans were created for each image, delivered to the moving phantom, and measured with a pinpoint chamber at the tumour centre. 3 fractions were delivered for each plan to minimise interplay.

**Results**

**Tumour motion range**

Median difference in tumour motion range (expected – measured) was 1.1 [0.1 – 1.9] cm (phase) and 1.3 [0.4-1.9] cm (amp.) (p=0.050).

**Density representation**

Median AIP HU profile agreement scores (ideal = 0) were 0.12 [0.05 – 0.42] (phase) and 0.13 [0.09 – 0.44] (amp.) (p=0.508).

**Dosimetry**

Dosimetric agreement between TPS and measurement is summarised in Figure 2. All amplitude-binned plans were measured within 2.5% of expected dose, compared with 9 of 10 phase-binned plans. The phase-binned outlier was an extremely slow breathing trace exceeding the pitch limits of our scanner. Median dosimetric agreement was not significantly different between methods (p=0.333).

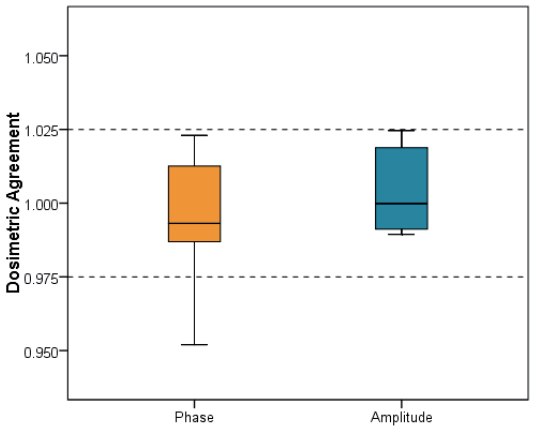


*Figure 2 Dosimetric agreement for VMAT plans (TPS vs measurement), phase-binned (left) and amplitude-binned (right). Dashed lines are ±2.5%.*

**Conclusion**

For the irregular breathing traces studied, no significant differences existed between phase and amplitude binning of 4DCT data regarding tumour motion range and average tumour density representation. Both methods slightly under-represented tumour motion but with appropriate PTV margins allowed for delivery of VMAT plans with acceptable dosimetric accuracy.

## OC-0414 Data mining in RT: Intrafraction motion and treatment time analysis for SBRT lung cancer patients

A. Licup[1], S. Nakhaee[1], S. Van Kranen[1], M. Rossi[1], F. Koetsveld[1], J.J. Sonke[1], P. Remeijer[1]
[1]*Netherlands Cancer Institute, Radiotherapy, Amsterdam, The Netherlands*

**Purpose or Objective**

Large scale analysis of patients' geometrical uncertainties is important to calculate appropriate margins and perform quality assurance. The common practice is manual, time-consuming collection of setup data. This study aims to demonstrate semi-automatic retrieval and analysis of large scale image registration data using data mining techniques. As a use case, the correlation between tumor and bone intrafraction (IF) motion of SBRT lung patients with treatment delivery times (TT) is investigated.

**Material and Methods**

We developed an in-house tool (ImStat) to allow for large scale retrospective analysis of setup data. First, ImStat queries patient-careplan information from a MOSAIQ® database and matches them to the online image database to retrieve the CBCTs (Elekta-XVI) and setup data. To facilitate automated analysis, we have introduced a labeling procedure to label the CBCTs according to a heuristic method. Four labels (prescan, inline, in-